Stability of Reshaping Breakwaters
with Special Reference to Stone Durability

P. Frigaard [1], T. Hald [1], H.F. Burcharth [1], Sigurdur Sigurdarson [2],

1 Introduction

Traditionally, conventional rubble mound breakwaters are designed with stable armour units, and consequently, very large stones or even artificial armour units are required. Reshaping breakwater designs allow reshaping of the seward slope thus involving stone movements. Ultimately, dependent on the degree of safety in the design, this reshaping process might end up in a stable profile where no changes in the cross sections occur even though stone movements are allowed.

Unfortunately, large movements of the protecting stones during the structural lifetime in combination with high stone velocities inherently cause some breakage and abrasion of the individual stones and thereby also reduced stability. In order to avoid excessive abrasion a high stone quality is demanded or larger stones must be applied when constructed. To allow the designer to account for abrasion and armour stone breakage due to the stone motion a description of the overall wave climate during the structural lifetime must be derived involving knowledge of transport rates, movement patterns, stone velocities and stone quality.

The main objective of the paper is to describe a tool enabling calculation of the anticipated armour stone movements. Also tensile stresses occur, as a result of stone against stone impact are discussed in order to make a more close connection between wave climate, stone movements and abrasion/breakage. Finally, a comparison to selected prototype structures is made to compare the armour stone movement model with visual profile observations of existing breakwaters.

[1] Hydraulics & Coastal Engineering Laboratory, Aalborg University, Sohngaardsholmsvej 57, DK-9000 Aalborg, Denmark, tel + 45 98158522, fax +45 98142555
[2] Icelandic Harbour Authority, Vesturvor, 2200 Kopavogur, Iceland

2 Longshore Transport Rate

Motion of stones along the active profile occurs when even slightly oblique waves attack the breakwater. This longshore motion has been evaluated in model tests performed by Burcharth and Frigaard (1988) and by van der Meer and Veldman (1992). Longshore transport was measured by observing the movements of stones layed out in coloured bands over the profile. To calculate the steady state transport the number of stones per wave passing a specific cross section at each sea state was divided by the number of waves. This ratio is termed the longshore transport rate S_x.

In Figure 1 the measured longshore transport rate is plotted against the mobility index $H_o T_{op} = \frac{H_s}{\Delta D_{n50}} T_p \sqrt{\frac{g}{D_{n50}}}$. The longshore transport rate seems to be described quite well by a power function as originally proposed by Vrijling (1991). The best fit of the power function to the data is:
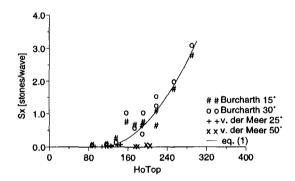
$$S_x = 85 \cdot 10^{-6} (H_o T_{op} - 105)^2 \tag{1}$$

Figure 1: Longshore transport rate for reshaping breakwaters.

One might argue if the model in eq. (1) is too simple because of the absence of obliquity. The model can however, easily be adjusted to include the angle of incidence θ as discussed by Alikhani et al. (1996). Though the effect of obliquity is small.

Another aspect of the transport model is the obvious sensitivity to the onset of motion. From the model it is seen that sea states slightly above those corresponding to the onset of motion result in significant transport due the rapid increase of the power function. The latter comparison with prototype breakwaters outlines this sensitivity.

3 Longshore Distribution of Transported Material

To characterize the motion of the individual stones on the breakwater several video recordings from the model tests performed by Burcharth and Frigaard (1988) have

been reanalysed thoroughly.

The main conclusion based on the analysis of the video recordings was a typical zigzag motion pattern as shown in Figure 2. The typical upward motion of the stone follows
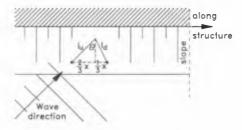

Figure 2: Typical pattern for single stone motion.

the wave direction θ whereas the downward motion is more controlled by gravity and an angle of half the angle of incidence seems more appropiate, see Figure 2. From Figure 2 the total travelled longshore distance can be calculated, assuming the upward and downward distances orthogonal to the structure in average are equal

$$l = l_u + l_d = \frac{2x}{3\sin(\theta)} + \frac{x}{3\sin(\frac{1}{2}\theta)} \qquad (2)$$

To quantify the travelled longshore distance x the longshore distribution of the transported material has been derived from the same tests. The longshore distribution was derived from recordings of the number of stones positioned in 5 cm wide bands over the profile along the entire length of breakwater. From these recordings the number of stones per m, the position of the individual stones and the mean stone movements are calculated. Figure 3 shows an example from a single longshore transport test.

Figure 3: Example of the longshore distribution of transported material.

In Figure 4 the longshore distribution is shown for all 22 tested wave conditions. As abscissa the travelled longshore distance x is normalized by the mean travelled distance $\bar{x}$ and as ordinate the stone distribution along the structure $s(x)$ (unit: stones/m per wave) is normalized by multiplying with $\frac{\bar{x}}{S_x}$.
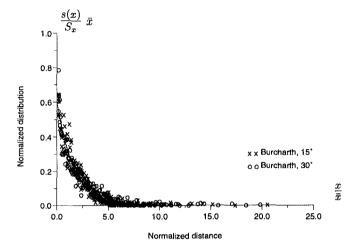

Figure 4: Longshore distribution of transported material.

From Figure 4 an excellent uniformity of the distribution curves for different wave climates and different angles of incidence is seen. Hence, a general exponential function can be fitted to the entire data set

$$s(x) = 0.6 \exp(-0.6\frac{x}{\bar{x}})\frac{S_x}{\bar{x}} \tag{3}$$

In Figure 5 the mean stone movement is plotted against the mobolity index for all 22 tested wave climates.

The mean stone movement is described by

$$\bar{x} = 5.3 \cdot 10^{-3} D_{n50}(H_o T_{op} - 105)\sin^{0.8}(2\theta) \tag{4}$$

or by inserting the longshore transport model eq. (1).

$$\bar{x} = 0.6 D_{n50}\sqrt{S_x}\sin^{0.8}(2\theta) \tag{5}$$

Inserting the mean travelled distance in the expression for l, eq. (3) gives the average distance moved per wave. Knowing the wave height/period scatter diagram describing the storm history for a specific area, it is possible to calculate the accumulated average distance moved by each single storm during the structural lifetime simply based on the easy accessible parameters, H_s, T_p, θ, number of waves and D_{n50}.

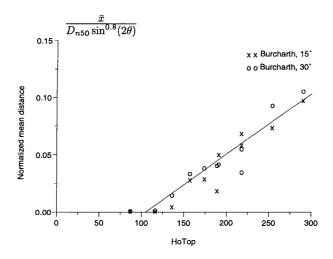$$\frac{\bar{x}}{D_{n50}\sin^{0.8}(2\theta)}$$

Figure 5: Mean stone movement versus the mobility index.

4 Impact Stresses in Armour Stones

A more close description than the stone motion connecting abrasion and breakage is to consider the tension stresses as a result of armour stones impacting armour stones during movements. This impact results in a shock wave propagating through the stone which is reflected at the edge structure resulting in a reverse propagating tensile stress wave. In case the tensile stress is too high the stone may crack depending on the stone quality.

In Figure 6 an idealized static model of a stone impact is sketched where the impacted stone remains at rest after impact. This is modelled by giving the stone infinity mass and zero velocity.

Applying Hertz' law to the system in Figure 6 results in the following equation
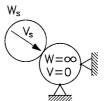

Figure 6: Static model

$$\sigma_{max} \propto \left(\frac{V_s^4}{D_{n50}}\right)^{0.2} E \tag{6}$$

where:

$$\begin{array}{ll} W_s & = \text{Stone weight} \\ V_s & = \text{Stone velocity} \\ D_{n50} & = \text{Nominal stone diameter} \\ E & = \text{Young's Modulus} \end{array}$$

Generally, eq. (6) describes the stresses with reason: a high velocity yields high stresses, a small diameter signifies large curvature and thus larger impact stresses because of the smaller contact area, and finally the elasticity of the stone is described by Young's Modulus. Another aspect is that by simple Froude scaling larger stones gain larger stresses.

From the previously described tests typical stone velocities during both run-up and run-down were investigated by video. A typical stone velocity during run-down equals the wave run-down velocity whereas the typical stone velocity during run-up is approximately 50-70% of the wave run-up velocity.

Several attempts to assess the run-up and run-down velocities have been made showing that the maximum expected velocity can be well described by H_s and $\xi = g(\alpha, H_s, T_p)$. The overall maximum velocity is expected to be in the order of $1.5\sqrt{gH_s}$, e.g. Sawaragi, (1995).

From the above considerations it seems that the impact stresses can be described by the same easy accessible parameters as the movement model. The model still needs verification and calibration to physical model tests as well as prototype measurements. More work has to be done into these subjects.

5 Comparison with Protoype Breakwaters

For prototype comparison four sites are investigated with wave and structural characteristics given in the two tables 1 and 2. The accumulated travelled mean distance have been calculated followingly:

- Calculation of longshore transport rate from eq. (1) for each storm.

- Calculation of mean position moved from eq. (5) for each storm.

- Calculation of total travelled distance from eq. (3) for each storm.

- Summation of total travelled distance during lifetime.

Regarding

1. Caldera, Costa Rica: Estimated stone movements are rather small indicating little stone movements during lifetime. Observations show little profile changes but some broken stones. This might be due to the very poor quality of the stones.

2. St. Paul, Alaska: Vast stone movements are estimated. Total damage of the breakwater was observed.

3. Racine, Wisconsin: Long travelled distance is estimated. Severe breakage and large profile changes were observed.

   4. Bolungarvik, Iceland: Little stone motions were estimated. Little profile changes
      observed.

It seems that the calculated distance corresponds very well to what might have happened.
Though, it is clear that actual damage depends on both the travelled distance and the
quality of the stones. In all, the comparison indicates that there is reason in relating
breakwater damage to the armour stone motion.

6   Conclusions

A model enabling calculation of the accumulated travelled stone distance is given based
on the easy accessible parameters such as H_s, T_p, θ, number of waves and D_{n50}. Fur-
thermore, a short discussion focusing on the structural integrity is given. It is argued
that the anticipated maximum tensile impact stresses can be evaluated by the same
easily accessible parameters, though more work need to be done into this subject.

A comparison with selected prototype structures is presented showing that there is
reason in relating breakwater damage to the armour stone motion. The comparison
also signifies that only little transport should be allowed in order to avoid severe damage.

In areas where sufficiently large armour stones can be difficult to get, the stone quality
is often poor. Even little stone transport or stone motion will in these cases result
in breakage and abrasion of the armour stones. In practice it is difficult to avoid
the abrasion and breakage of the armour stones and thus little transport should be
allowed. The best possible design of the berm breakwater with maximum utilization
of the quarry when possible is suggested by Sigurdarson et al. (1995). The aim is to
minimize stone movements and make a more or less statically stable structure with little
expected movements during the lifetime if suitable quarries are found in the vicinity.
Still if stone movements occur on the berm breakwater no abrupt failure occur. By the
berm concept up to 100% of the quarry yield can be used. This design approach have
been used videly in Iceland with succes, see Sigurdarson and Viggosson (1994).

7   Acknowledgement

8   References

Alikhani, A., Tomasicchio, R. and Juhl, J., *Berm Breakwater Trunk Exposed to Oblique Waves*, to be published in Proc. 25th ICCE, Orlando, USA, 1996.

Burcharth, H.F., Frigaard, P., *On 3-Dimensional Stability of Reshaping Breakwaters*, Proc. 21th ICCE, Malaga, Spain, 1988.

CIRIA/CUR, *Manual on the Use of Rock in Coastal and Shoreline Engineering*, Published jointly by the Construction Industry Research and Information Association in the UK and the Centre for Civil Engineering Research, Codes and Specifications in the Netherlands, 1991.

Lamberti, A., Tomasicchio, G.R., *Stone Mobility and Abrasion on Reshaping Breakwaters* to be published in Coastal Engineering, 1996.

van der Meer, J.W., Veldman, J., *Singular Points at Berm Breakwaters: Scale Effects, Rear, Round Head and Longshore Transport*, Coastal Engineering, Vol. 17, Nos. 3,4, August 1992.

Vrijling, J.K., Smit, E.S.P. and Swart, P.F., *Berm Breakwater Design; the Longshore Transport Case: a Probabilistic Approach*, ICE, Proc. Coastal Structures and Breakwaters, London, 1991.

Sawaragi, T., *Coastal Engineering – Waves, Beaches, Wave–Structure Interactions*, Developments in Geotechnical Engineering, 78, Elsevier Science B.V., 1995.

Sigurdarson, S., Viggosson, G., *Berm Breakwaters in Iceland, Practical Experiences*, Proc. Int. Conf. on Hydro-Technical Engineering for Port and Harbour Construction, Yokosuka, Japan, October 1994.

Sigurdarson, S., Viggosson, G., Benediktsson, S., Samarason, O. B. *Berm Breakwaters and Quarry Investigations in Iceland*, Proc. 4th Int. Conf. on Coastal & Port Engineering in Developing Countries, Rio de Janeiro, Brazil, September 1995.

Location	W_{50} [t]	ρ [t/m³]	storm	duration [waves]	H_s [m]	T_p [sec]	Θ [deg]	H_0	$H_0 T_{0p}$	S [stones/wave]	l_i [m]
Caldera, Costa Rica	5.0	2.40	21.09.78	3000	3.65	18.7	50	2.1	109.5	$1.7\ 10^{-3}$	155
	5.0	2.40	21.05.81	3000	3.55	17.9	50	2.1	101.2	0	0
	5.0	2.40	18.07.83	3000	3.47	17.1	50	2.0	95.2	0	0
	5.0	2.40	18.06.78	3000	3.30	17.5	50	1.9	92.6	0	0
St. Paul, Alaska	1.5	2.77	13.11.84	1900	5.34	31.0	15	3.8	417.1	8.3	7886
	1.5	2.77	07.12.84	4000	5.34	15.0	15	3.8	201.8	0.8	5155
Racine, Wisconsin	0.82	2.61	08.03.87	2500	4.4	11.2	15	4.15	176.6	0.4	1984
Bolungarvik, Iceland	6.0	2.85	27.10.95	3000	6.0	15	10	2.65	109.9	$2.0\ 10^{-3}$	338

Tabel 1: Experienced wave conditions and structural parameters for selected prototype structrures.

Location	St. type/shape	W_{50} [t]	ρ [t/m³]	$\frac{W_{85}}{W_{15}}$	$H_{0,max}$	$H_0 T_{0p,max}$	S_{max} [st./wave]	$\sum l_i$ [m]	Visual profile observations
Caldera, Costa Rica	Sand stone/Rough angular	5.0	2.40	1.5	2.1	110	$1.7\ 10^{-3}$	155	app. 5-10% broken stones, severe abrasion little profile changes and longshore transport.
St. Paul, Alaska	Crushed stone	1.5	2.77	3.0	3.8	417.1	8.3	13041	total damage, 150 m recession of breakwater head.
Racine, Wisconsin	Crushed limestone	0.82	2.61	2.5	4.15	176.6	0.4	1984	severe breakage of armour stones, large profile changes and longshore transport.
Bolungarvik, Iceland	Quarry stone/Rough angular	6.0	2.85	2.5	2.65	109.9	$2.0\ 10^{-3}$	338	no armour stone breakage, little profile changes, no longshore transport.

Tabel 2: Comparison of experienced wave conditions, structural parameters and profile observations for selected prototype structrures.
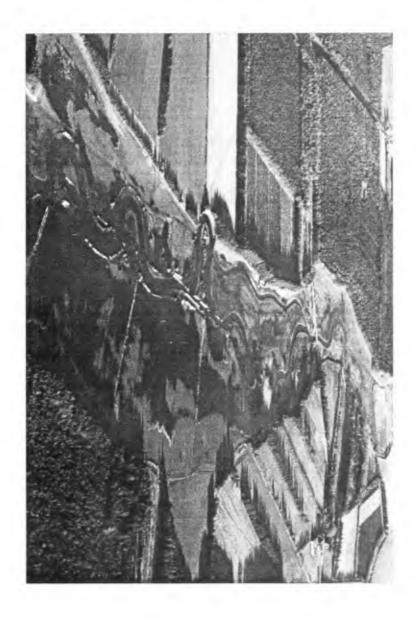
Photo from Icelandic berm breakwater

Photo from Norwegian berm breakwater